



Geotechnical behavior of high-plastic clays treated with biopolymer: macro–micro-study

Muhammad Hamza^{1,2} · Zhihong Nie¹ · Mubashir Aziz^{3,4} · Nauman Ijaz⁵ · Osama Akram² · Chuanfeng Fang¹ · Muhammad Usman Ghani⁶ · Zain Ijaz⁵ · Sadaf Noshin² · Muhammad Faizan Madni⁷

Received: 14 June 2022 / Accepted: 14 January 2023 / Published online: 3 February 2023
© The Author(s), under exclusive licence to Springer-Verlag GmbH Germany, part of Springer Nature 2023

Abstract

The quantification of long-term performance of mechanically/chemically treated problematic soils is still under discussion. Likewise, exploring the availability and use of eco-friendly and sustainable stabilizing admixtures is a parallel area of contemporary research. This paper presents the laboratory results of a highly plastic soil strengthened with xanthan gum (*XG*) biopolymer to determine its suitability as a suitable subgrade for pavements. The *XG* content varied from 0 to 5 percent, and the specimens were tested at different aging periods (0–60 days). The unconfined compressive strength (*UCS*) of soil strengthened with 1.5% *XG* content showed a considerable enhancement in strength by 314 percent, strength improvement ratio (*SRI*) increased by 8.3 times, and energy absorption capacity (E_v) by 1.4 times, resulting in a hard-quality subgrade for pavement construction. The compression (C_c) and rebound (C_s) indices were greatly reduced by 78 percent, as well as the swell potential parameters (percent swell (S_w) and swell pressure (S_p)) were decreased by 85 percent on average. The hydraulic conductivity of treated soil as well as the moisture-mass losses in freeze–thaw durability test was also found to be greatly enhanced with increased *XG* content. Aging time also plays a pivotal role in enhancing the strength and anti-deformation characteristics of stabilized soil up to 60 days. *SEM* coupled with *EDX* analysis proved the aggregation of soil particles by hydro-gelling effect of biopolymer, which helps in the improvement of strength and durability. Therefore, *XG* biopolymer has a promising potential as an alternative admixture for treating widespread fat subgrade soils.

Keywords Highly plastic soil · Xanthan gum · Unconfined compressive strength · Strength improvement ratio · Hydraulic conductivity · Freeze–thaw durability

Introduction

Expansive clays with low shear strength and high compressibility are common in many parts of the world, especially in tropical areas like Pakistan (Ali et al. 2020), Australia, Thailand, and Malaysia. These clays beneath foundations and pavements are generally related to undesirable lateral movements on loading, differential settlement issues, and bearing capacity problems (Ijaz et al. 2022b). Therefore, soil stabilization methods are commonly suggested for these clays (Hamza et al. 2022b). Soil improvement techniques are generally classified as either mechanical or chemical; in certain circumstances, a mix of treatments is also applied. Commonly known mechanical improvement methods include

soil reinforcement (Hamza et al. 2022a), densification, and dewatering.

On the other hand, chemical techniques and biological methods involve the stabilization of weak soils by chemical admixtures and biotic processes (Hamza et al. 2022c). Conventional chemical admixtures like fly ash, bituminous materials, lime, calcium, carbide, and cement are used in the construction industry nowadays (Aziz et al. 2022, 2021). Though these chemical admixtures offer many benefits like workability, hydraulicity, enhanced durability, and high strength at a reasonable price (Ijaz et al. 2020, 2022a; Aziz 2020), they leave an irreparable and everlasting mark on the environmental ecosystem. Cement is a commonly used material and popular soil stabilizer that releases half tons of carbon dioxide (CO_2) gas for each ton of its production (Latifi et al. 2016a, b), as well as it accounts for about 5 percent of global CO_2 gas emissions (Chang et al. 2016). Also, nitrogen oxides are produced in cement production

✉ Muhammad Hamza
enr.hamza30@gmail.com

Extended author information available on the last page of the article

kilns in addition to CO₂ emissions. Moreover, the conventional admixtures change the *pH* of the treated soil, affecting vegetal and groundwater quality and contributing to desertification. Likewise, it has been observed that the soil treated with chemical admixtures shows brittle behavior, which reduces the overall structural stability (Sujatha et al. 2021). Ecological concerns and the requirement for sustainable growth necessitate using an environmentally friendly stabilizing material. Therefore, natural admixtures such as powdered glass, plastic, paper, fibers, and biopolymer are becoming popular for the economic treatment of high-plastic soils (Latifi et al. 2017).

Being derived from natural processes, biopolymers such as xanthan gum, gellan gum, guar gum, alginate, chitosan, polyurethane resin, agar, and polyglutamic acid can substitute conventional admixtures as soil stabilizers (Kumar and Sujatha 2020). It also finds application in slope strengthening, erosion control, soil stabilization, liquefaction mitigation, and bioremediation (Hamza et al. 2022d). Biopolymers do not contribute to harmful gas emissions owing to the carbon-capture effect in the production phase, resulting in a negligible carbon dioxide trace, and therefore branded as sustainable, carbon-neutral, and environmentally friendly materials (Lee et al. 2019). Biopolymers are natural polysaccharides produced by algae, bacteria, and fungi that have inherent properties like pseudo-plasticity, stability, resistance to shear breakdown, and high viscosity throughout a wide range of temperatures and pH (Moghal and Vydehi 2021). Xanthan gum (XG) biopolymer is now the most commonly used anionic biopolymer for generating biodegradable polysaccharides (Petri 2015), synthesized by bacterial micro-organisms *Xanthomonas campestris* using carbohydrate as the main raw material. XG is non-toxic, odorless, water-soluble, low cost, and shows advanced stability in temperature, salt, base stability, and acid, accompanied by good resistance to oxidation and enzymatic hydrolysis (Rosalam and England 2006).

Elkafoury & Azzam (2021) evaluated the performance of XG-amended fine sand and observed that the CBR value of treated soil improved by three times with 0.9% XG compared to natural soil. The tensile strength of low-plastic clay treated with xanthan and guar gum increased by 25 and 10 times, cohesion increased by 5 and 1.5 times, and friction angle reduced by 2° and 12°, respectively (Soldo et al. 2020). The dehydration of gum causes biopolymer gel to change to a glassy state, which accumulates inside the pore spaces of clay particles and strongly binds them together to form a crosslinking network, thus improving the unconfined shear strength (Acharya et al. 2017; Arasan et al. 2017; Latifi et al. 2016a, b), deviatoric stress (Soldo et al. 2020), cohesion with friction angle (Ayeldeen et al. 2016; Dehghan et al. 2019; Latifi et al. 2017), California bearing strength (Chen et al. 2013, 2015), permeability with hydraulic conductivity

(Ayeldeen et al. 2017; Biju & Arnepalli 2020; Cabalar et al. 2017; Muguda et al. 2017), Atterberg limits with compression index (Nugent et al. 2011, 2009), and metal uptake capacity with leachability. Because of their benefits and prospective properties, these biopolymeric stabilizers have been recognized as viable soil strengthening additives with significant potential in various areas of the construction industry. Table 1 summarizes the recent research findings related to biopolymeric stabilization of weak geomaterials.

Though, most of the research known in the literature was mainly focused on low-plastic, silty clays, residual, and sandy soils with limited work on problematic high-plastic clays. Besides, understanding XG-stabilization corresponding to freeze–thaw durability performance also requires special attention to pave its path for practical field implementations. Therefore, a comprehensive study is needed to highlight and understand the potential attributes of XG-treatment of problematic high-plastic clay with particular attention to subgrade strength which involves specialized testing considering the freeze–thaw durability performance. Such studies are deemed necessary as they provide a sustainable and environment-friendly solution and pave the way for future field applications.

Considering the discussion, this study aimed to explore the mechanical behavior of XG-treated problematic high-plastic clay with particular attention to subgrade tests, coupled with microstructural and elemental testing to understand the possible interaction mechanism of XG with high-plastic clays by incorporating long-term aging conditions. This comprehensive study will provide the scientific basis and better understanding of the long-term behavior of XG-treatment of problematic high-plastic subgrade to researchers and practitioners working in a similar research area. Macroscale tests performed to determine the mechanical behavior of natural and treated soils include unconfined compression strength (*UCS*), direct shear (*DS*), swell-consolidation, permeability, and freeze–thaw durability tests. Microscale tests conducted to examine the micro-level changes in treated soil include scanning electron microscopy (*SEM*), energy-dispersive x-ray (*EDX*), and Brunauer–Emmett–Teller (*N₂-BET*) surface area analyses. Furthermore, tests were performed on treated samples at prolonged aging (0–60 days) to investigate the changes in mechanical strength and microlevel properties of the treated soil over time.

Materials and methods

Natural soil and xanthan gum biopolymer

The natural soil used in this research was quarried from 2 to 3.5 m below the ground level from Kohat district in

Table 1 Literature review on the utilization of different biopolymers for soil amelioration

Reported by	Soil type	Biopolymer type	Optimum quantity	Experimental results
Present study	Highly plastic clay	Xanthan gum	1.5%	Enhancement in unconfined and direct shear strengths, anti-deformation properties, and mitigation of swelling potential
Wang et al. (2021)	Red clay	Xanthan gum	1.5%	Strength enhancement, and improvement in cohesion and internal friction angle
Kumar and Sujatha (2021)	Silty clay	Xanthan gum	1%	Strength enhancement, considerable reduction in hydraulic conductivity
Bağrıaçık and Mahmutluoğlu (2021)	Clean sand	Xanthan gum	1.25%	Improvement in bearing capacity
Kumar and Sujatha (2020)	Clayey sand	βeta-glucan	–	Strength enhancement
Soldo et al. (2020)	Sand with silt	Xanthan gum, βeta-1,3/1,6 glucan, Chitosan, Guar gum, and Alginate	2% XG and 1% GG	Strength enhancement
Soldo and Miletić (2019)	Silty sand	Xanthan gum	1%	Strength enhancement
Chen et al. (2019)	Sand	Xanthan gum	–	Drying leads to increase strength and cohesion
Lee et al. (2019)	Sand	Xanthan gum	2%	Strength enhancement
Kwon et al. (2019)	Marine clay	Xanthan gum, ε-polylysine	2%	Strength enhancement
Dehghan et al. (2019)	Silty clay	Xanthan gum	2%	Decrease in permeability and collapsible potential
Chang and Cho (2019)	Sand-clay mixtures	Gellan gum	1%	Increase in the shear strength parameters

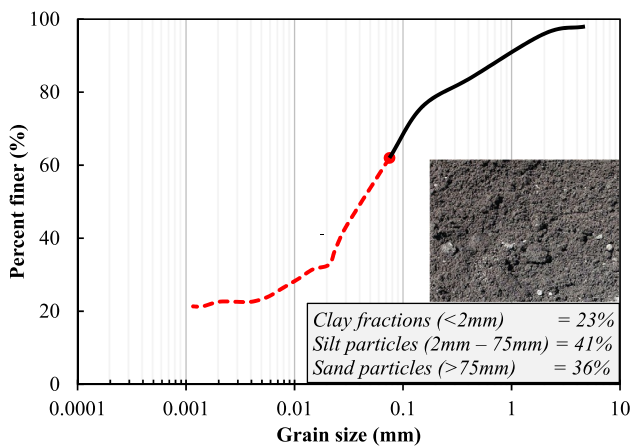


Fig. 1 Grain size distribution curve of natural soil

Khyber Pakhtunkhwa, Pakistan, with geographical coordinates (33°33'57.6" N, 71°29'30.0" E). The soil comprises 36 percent sand, 41 percent silt, and 23 percent clay contents (Zamin et al. 2021), as shown by the gradation curve in Fig. 1. The liquid limit is 50.5 percent, the plasticity index is 30.5 percent, plastic limit is 20 percent, specific gravity is 2.68, and classified as high-plastic clay or fat clay (CH) according to the Unified Soil Classification System (USCS). X-ray diffractogram (XRD) of pure soil shows the dominant

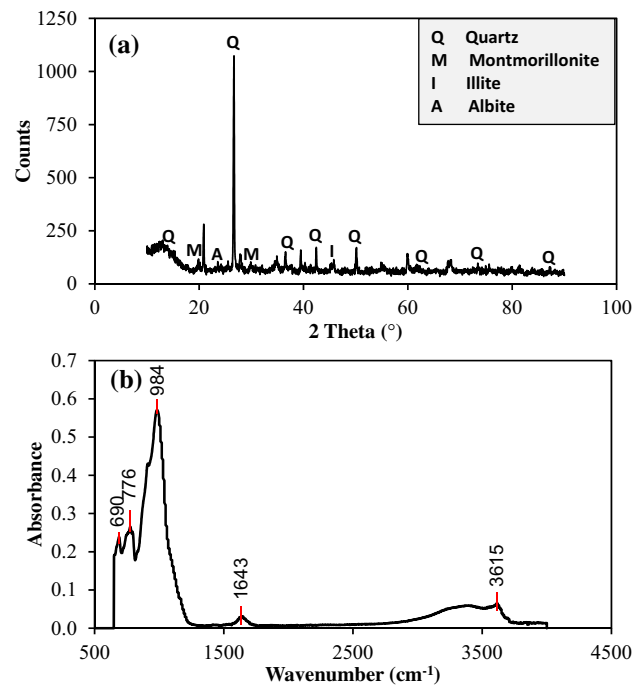


Fig. 2 a XRD, and b FTIR spectra of natural soil

presence of quartz mineral, while swelling clay minerals (montmorillonite, illite) are also present in the soil sample as shown in Fig. 2a. The Fourier-transform infrared spectroscopy (FTIR) of the natural soil is presented in Fig. 2b. The bending and stretching vibrations recorded in FTIR spectra revealed the presence of Al–OH, Si–OH, and Mg–OH groups.

Xanthan gum biopolymer, a natural polysaccharide generated by the microbe *Xanthomonas campestris* (Garcia-Ochoa et al. 2000), was used in this study for soil stabilization purpose. The most often used microbe for the commercial synthesis of xanthan gum, *Xanthomonas campestris*, is an aerobic bacterium, and fermentation results in a significant rise in viscosity (Rosalam and England 2006). Therefore, xanthan gum solutions have high shear stability and higher pseudo-plasticity. Because of these qualities, xanthan gum has a wide range of uses in the pharmaceutical, oil, paint, food, cosmetic, textile, and paper industries as a thickening, suspending, gelling, viscosity controller, or as a flocculant (Comba and Sethi 2009). XG looks like a dry and cream-colored powder with grain size passing *American Society for Testing and Materials* (ASTM) #200 mesh. It is water soluble, viscosity of 1615 cps, anionic charge, and specific gravity of 1.1.

The SEM and EDX of natural soil and xanthan gum are presented in Fig. 3. The soil SEM demonstrates the presence of voids and micro-cracks in its microstructure (Fig. 3a), which would impact strength and deformation behavior when subjected to moisture fluctuations in the field. It also shows platy soil grains stacked in a parallel configuration to produce a dispersed structure. The microstructure of pure

XG presents a continuous and smooth surface with fiber matrices in Fig. 3b. The EDX of pure soil shows the elemental composition as oxygen (O-47%), carbon (C-14%), silicon (Si-18%), aluminum (Al-8%), and EDX of xanthan gum comprises oxygen (O-39%) and carbon (C-55%) with trace amounts of other elements.

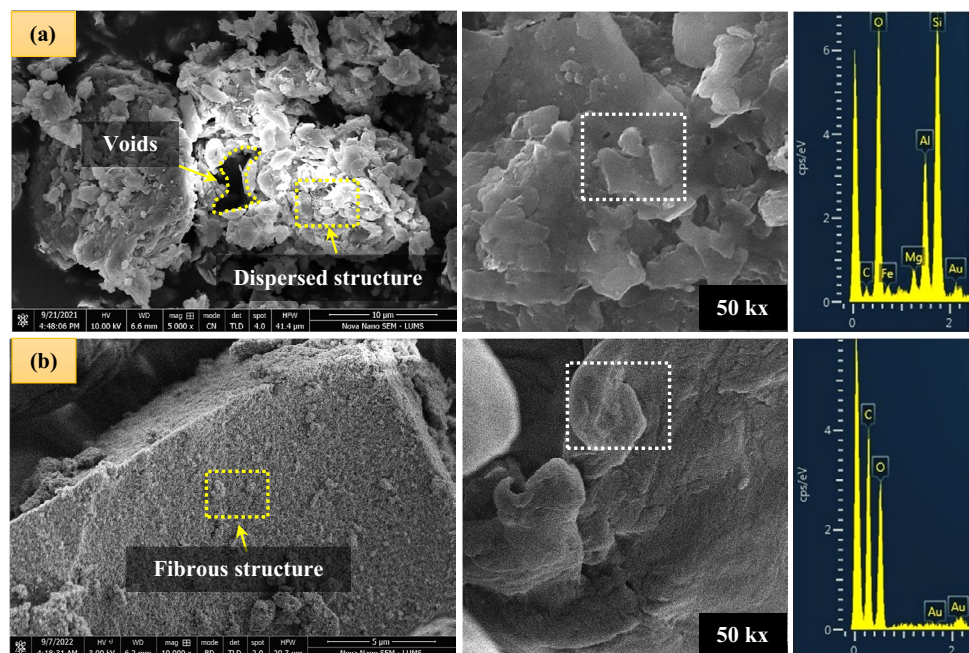
Specimen preparation and testing program

The XG biopolymer was mixed in natural soil at 0, 0.5, 1, 1.5, 2, and 5 percent of the soil's dry mass, which is the most acceptable method for field application. The prepared mixtures were placed in sealed plastic bags for 24 h to achieve a homogeneous moisture distribution. The soil-XG mixtures were subjected to naturally air-dried aging conditions for an aging of 0, 4, 7, 14, 28, and 60 days for the performance of geotechnical experimentation as presented below.

Tests for mechanical behavior

Unconfined compression tests were conducted according to ASTM D2166M-16 on treated soil specimens compacted at their respective maximum dry density (MDD) and optimum moisture content (OMC) in the split mold of 38 mm diameter and 76 mm height. The samples were kept in plastic bags at 25 °C during the required aging periods of 0, 4, 7, 14, 28, and 60 days. A strain-controlled UCS apparatus was used to apply uniaxial compression load at a strain rate of 1.27 mm/min to a maximum of 20 percent strain. Direct shear tests were carried out using standard shear box apparatus (20 mm height and 60 mm

Fig. 3 SEM with EDX graphs of powdered samples **a** natural soil, and **b** xanthan gum



sides) according to ASTM D3080. The samples were tested at three different normal stresses at a 1.0 mm/min horizontal displacement. It is appropriate to mention here that for the *UCS* and direct shear tests, the soil was mixed with the desired biopolymer percentage at their respective optimum moisture contents (OMCs) overnight at a room temperature of $(28 \pm 2 \text{ }^\circ\text{C})$ and compacted at maximum dry densities (MDDs).

One-dimensional consolidation tests were conducted according to ASTM D2435M-11 on the treated specimens of 75 mm diameter and 20 mm height. An initial seating load of 2.5 kPa was applied to prevent swelling of the soil, and after that, the applied vertical load was maintained for 24 h until there was no further change in vertical strain. The load increments of 10, 20, 50, 100, 200, 400 and 800 kPa were applied at elapsed times of 0.25, 1, 2.5, 4, 6.25, 9, 16, 25, 30 min, 1 h, 2, 4, 8, and 24 h.

A series of falling head permeability tests were also conducted according to ASTM D5084. For this purpose, the required quantity of soil, water, and xanthan gum were hand mixed to achieve a homogeneous mixture and compacted using a standard Proctor mold (ASTM D698-12). The soil samples were saturated by soaking in water, and the permeability values were recorded over 120 h. The durability performance of soil was studied by conducting cyclic freeze–thaw tests in line with (ASTM D560 2012), and soil samples were prepared with XG content (0, 0.5, 1, and 1.5%). Three sets of samples were prepared for each mix to calculate the moisture content and mass losses. For this purpose, the soil samples were covered in a polyethylene bag and kept for ten aging days in a damp chamber. The test was then executed for 12 successive cycles when the aging process was over.

Tests for microstructural analysis

The microstructural behavior of the soil specimens was elucidated through *SEM*, *EDX*, and *BET* surface area analyses. Field-emission scanning electron microscope (Nova NanoSEM 450) was used for microscopic examination (state, shape, and size of aggregation, arrangement of particles, etc.) of the treated soil matrix. This test also helped detect the formation of new cementitious hydrogels that are difficult to identify with other microstructural characterization methods. Each dried soil specimen was positioned on an aluminum stub covered with two-sided carbon tape and coated by gold (*Au*) sputtering for 110 s at 25 milliamperes under a high vacuum until it was fully covered and ready for *SEM* analysis. The *EDX* analysis was also used with *SEM* to determine the elemental composition of the soil samples. The change in surface area of the particles of XG-treated soils offers helpful insight into the physical changes and chemical reactions during the treatment process. Likewise, *BET* surface area analysis was also used to estimate the surface area of test materials.

The test specifications and specimen details and their associated references are summarized in Table 2.

Results and discussion

Effect of XG on compaction properties

Figure 4 shows the variation in *MDD* and optimal water content *OMC* with xanthan gum. It can be observed that the *MDD* and *OMC* values of natural soil and XG-treated soil differ significantly. *MDD* of natural soil was around 18.7

Table 2 Test specifications

Test	Test parameters in SI units	Specimen details	References
Compaction test	<i>MDD</i> (kN/m^3) and <i>OMC</i> (%)	0.102 m (dia.) \times 0.1161 m (ht.)	ASTM D698–12 (2021), ASTMD(1557)–12e1 (2012)
Unconfined shear strength test	<i>UCS</i> (kPa) <i>E</i> ₅₀ (kPa)	0.0381 m (dia.) \times 0.0762 m (ht.)	ASTM D(2166)M–16 (2016) Chang et al. (2015)
Direct shear test	<i>c</i> (kPa) and ϕ ($^\circ$)	0.02 m (ht.) \times 0.06 m (sides)	ASTM D3080 (2011)
Consolidation test	<i>C</i> _c , <i>C</i> _s , <i>S</i> _w (%), and <i>S</i> _p (kPa)	0.075 m (dia.) \times 0.02 m (ht.)	ASTM D (2435)M–11 (2011)
Permeability test	<i>k</i> ($\times 10^{-7}$ cm/s)	0.1 m (dia.) \times 0.1273 m (ht.)	ASTM D5084 (2016)
Freeze–thaw durability test	Mass loss (%) and moisture loss (%)	0.1016 m (dia.) and $1.1\text{E-}5 \text{ m}^3$ (vol.)	ASTM D560
X-rays diffraction analysis	Mineralogical composition	Powdered form	Advance Bruker D8 diffractometer
Fourier-transform infrared spectroscopy test	Infrared absorption spectra	Powdered form	IRTracer-100FTIR spectrometer
BET surface area analysis	Surface area (m^2/g)	0.5–2 g soil and 9 mm glass cells	Horiba SA-9600
Energy dispersive x-ray analysis	Elemental composition	Powdered form	Nova NanoSEM 450
Scanning electron microscopic analysis	Microstructure arrangement	$1\text{E-}6 \text{ (m}^3)$	

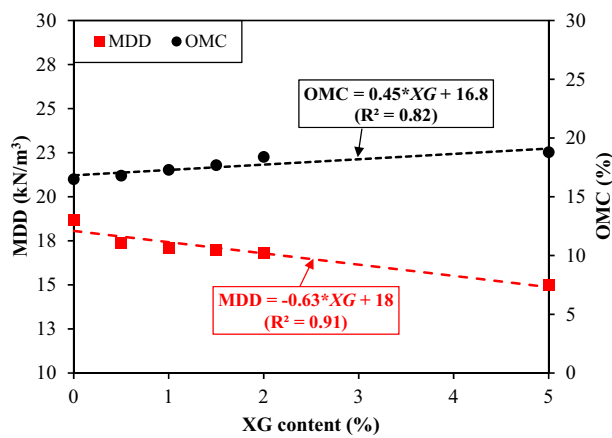


Fig. 4 Compaction characteristics of XG-treated soil

kN/m³, and the *OMC* was 16.5 percent which was changed to 15 kN/m³ and 18.8 percent, respectively, at an XG content of 5 percent. These compaction characteristics emerged from changes in sample properties and water absorption of hydrophilic XG biopolymer. The subgrade construction material should have a dry unit weight of at least 16.5 kN/m³ (Congress 2015), so the samples prepared at modified Proctor densities meet this criterion satisfactorily. Soil and granular materials should be compacted to max dry density; otherwise, poor pavement performance will result.

Effect of XG on consolidation—swell behavior

The consolidation-swell behavior of soil treated with different percentages of XG at aging periods (0–60 days) is represented by various parameters such as compression index (*C_c*), rebound index (*C_s*), swell pressure (*S_p*), and percent swell (*S_w*), as shown in Fig. 5. The *C_c* and *C_s* values of soil containing 1.5% XG were initially increased by 10 and 47 percent at 0 day of aging due to the natural expansivity of the XG hydrogels. But with the application of prolonged aging of 60 days, both parameters were significantly reduced by 78% on average as shown in Figs. 5a, b. The obtained *C_c* value for 1.5% XG-stabilized soil (i.e., 6%) is well below the permissible limit (<13%) for low expansive soil (Holtz and Gibbs 1956). Hence treated soil became stiffer with time due to the formation of cementitious hydrogel networks and offered excellent resistance to the settlement of soil structure caused by an external load. Similar behavior has been observed for other XG percentages and aging periods. Researchers (Latifi et al. 2017; Singh and Das 2020) observed similar compression and rebound indices trends with the addition of XG content. Consistent with the UCS results, the most substantial improvements in strength behavior were noticed in the first 28 days of aging, with nearly little change reported between 28 and 60 days. The effect

of XG addition on the soil swelling potential (*S_w*, *S_p*) with prolonged aging is presented in Fig. 5c, d. The maximum swell percentage of pure soil is 5 percent, and this swelling is mainly due to the presence of montmorillonite or illite minerals in the soil. Including 1.5 percent XG content in pure soil significantly reduced the swell percent by 76 percent (from 5 to 1.2 percent) for 28 days and further reduced it to 82 percent (up to 0.9%) for an aging period of 60 days as compared to virgin soil. Thus, the expansivity of stabilized soil was changed from medium class to low class after an aging time of 28 days, as its percentage swell is well below the permissible limit of 1.5% (Hamidi and Hooresfand 2013). Also, the swell percent is below the acceptable limit of 2% as specified by the Housing and Urban Development (HUD) Department of America (Day 2006). Likewise, the swell pressure of soil with 1.5 percent XG was reduced by 82 percent (from 103 to 19 kPa) for 28 days and 86 percent (from 103 to 14 kPa) for 60 days of aging, which is also within the permissible range of 50 kPa for low swelling class (McCormack 1976). Prolonged aging also influences the swell potential due to the presence of hydrogel in soil fabric, which offers excellent resistance to its volumetric expansion.

Prediction models for *C_c*, *C_s*, *S_w*, and *S_p* of treated soil

Based on the consolidation test results presented in this study, regression analysis was performed to develop a prediction model for the percent decrease in swell-consolidation parameters of treated soil, as shown in Fig. 6. The prediction models with the relevant statistical coefficients have been presented in Table 3. Proposed prediction models fit the observed data well, with regression (*R*²) values of 80, 84, 88, and 82 percent, respectively, as presented in Eqs. (1–4):

$$\Delta C_c = 15.8 + 1.9 \times XG + 1.1 \times d [R^2 = 0.80] \tag{1}$$

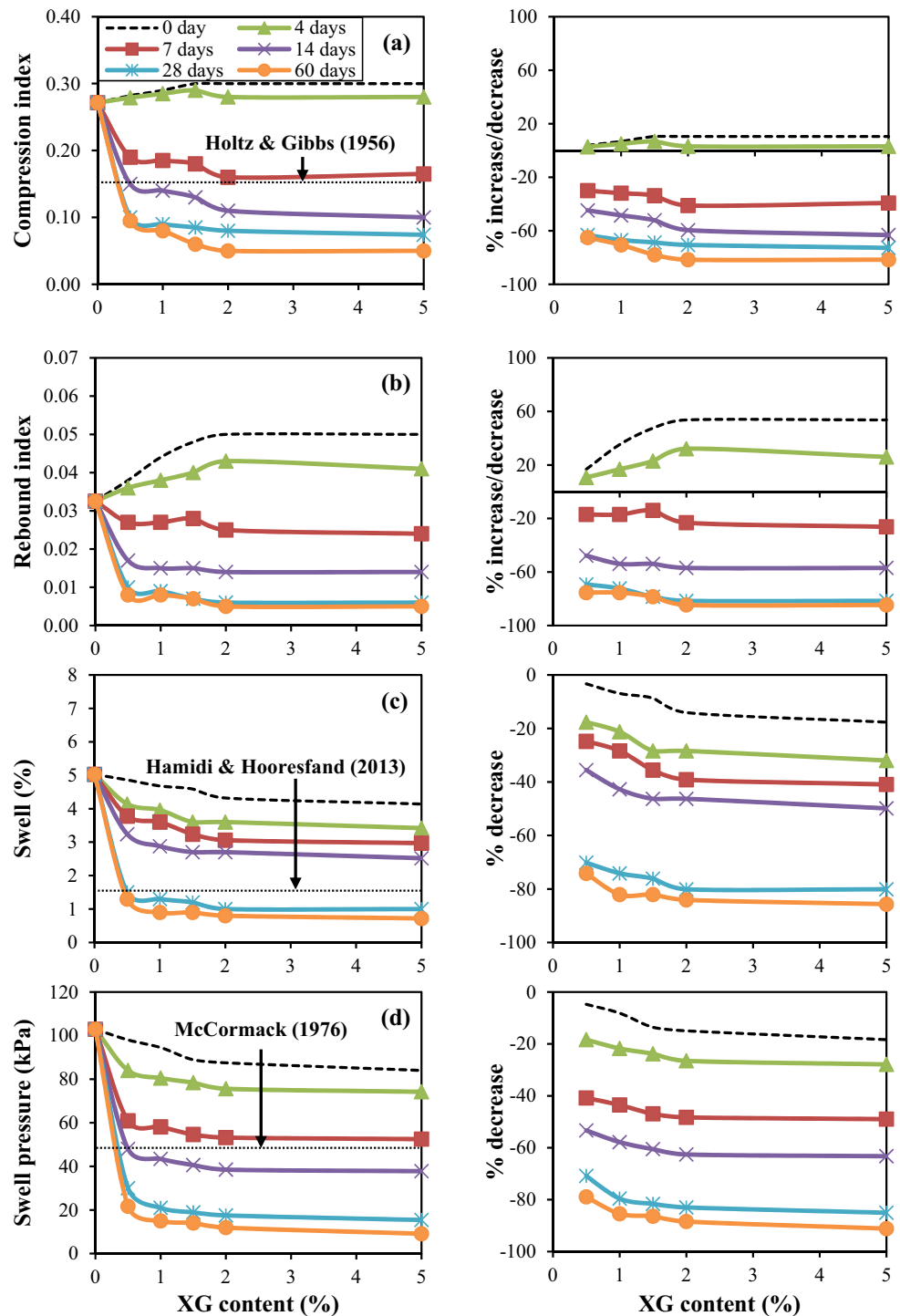
$$\Delta C_s = 25.2 + 2.8 \times XG + 0.9 \times d [R^2 = 0.84] \tag{2}$$

$$\Delta S_w = 16.1 + 2.8 \times XG + 1.0 \times d [R^2 = 0.88] \tag{3}$$

$$\Delta S_p = 26 + 1.9 \times XG + 1.1 \times d [R^2 = 0.82] \tag{4}$$

where *C_c* denotes compression index, *C_s* denotes rebound index, *S_w* denotes percentage swell, and *S_p* denotes swell pressure, given that the predicted decrease of *C_c*, *C_s*, *S_w*, and *S_p* of soil depends on the variations in the percentage of xanthan gum (*XG*) and aging time (*d*) in stabilized clay. Therefore, the independent variables selected to predict the empirical model in this study include the additive content (*XG*) and the aging time. The significance associated P-value (*Significance F*) for

Fig. 5 Comparison of swell-consolidation parameters and percentage increase/decrease **a** compression index, **b** rebound index, **c** percent swell, and **d** swell pressure



all prediction models is less than the tolerable limit of 0.05. Moreover, it has been observed that about 92% of the data points fall within the range of 90% upper–lower prediction bands, which show reasonably good prediction models.

Effect of XG on shear strength parameters of soil and its strengthening mechanism

In UCS testing, the prepared soil specimens were allowed to dry until the required aging period to allow a complete chemical reaction between the soil and XG polymer. Even a

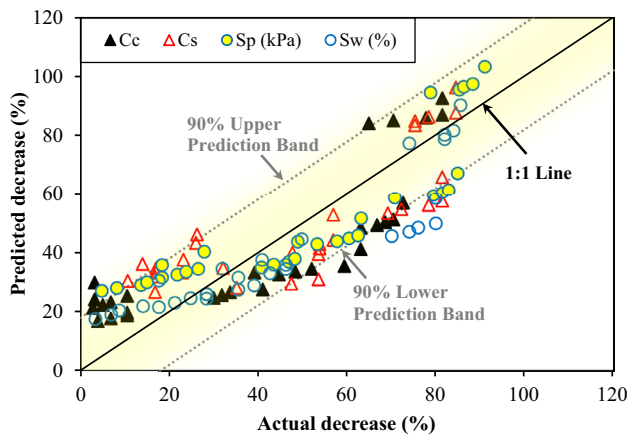


Fig. 6 Prediction model for swell-consolidation parameters of treated soil

small percentage of XG showed a significant improvement in UCS (Fig. 7a) because the XG biopolymers have high specific surfaces that allow for extensive contact between soil particles, resulting in a hard soil matrix with increased strength. Significant effects of both XG content and the aging period on UCS of the treated soil were observed. The testing was conducted at a maximum of 60 days of aging and 5 percent XG since no further strength enhancement was observed beyond these limits. The subgrade quality of clay stabilized with 1.5 percent XG altered from medium to hard quality, as its UCS of 728 kPa is much larger than the minimum requirement of 360 kPa for a subgrade of hard quality (Das and Sobhan 2013). The UCS of treated soil is also within the suitable range of 687 to 1373 kPa for good quality subgrade (Ingles and Metcalf 1972). The Strength Improvement Ratio (SIR) for the unconfined compressive strength of the XG-treated soil specimens is presented in Fig. 7b, and can be determined using the following equation;

$$SIR = \frac{\text{Improved Unconfined Compressive Strength}}{\text{Initial Unconfined Compressive Strength}} \quad (5)$$

The formation of hydrogels that bind the soil grains together and fill the pore spaces in the samples can explain the increase of compressive strength over time (Latifi et al.

2016a, b). The anionic XG biopolymer, in unification with soil particles, provides significant viscose forms, improving the ductility of soil samples. Interestingly, similar behavior has been observed for sand treated with polypropylene fiber reinforcement, transforming its brittle behavior into a relatively ductile one (Hamidi and Hooresfand 2013). Polysaccharides were thought to work by having high absorption and strong microstructural interaction in the samples (Chenu 1993). Chang et al. (2015) showed that the microstructural interactions between the XG gels and soil grains improve grain-to-grain contact. Accordingly, the E_v of the samples tested was calculated by carrying out the derivation of the area under the stress–strain curve up to the peak point. XG inclusion into soil increased E_v ; thus, the materials were intended to deal with the problems of inelastic response to large dynamic loads, as in Fig. 7c.

BET surface area analysis

When evaluating the physical interaction of clays stabilized with biopolymer additions, the specific surface area is a crucial attribute to understand. Figure 8 depicts the results of BET testing on natural and xanthan gum biopolymer-treated soils with varying aging time intervals. As indicated, increasing the aging time resulted in a significant reduction in the surface area of the treated samples. The flocculation of soil grains to form greater soil clusters during cementation reduces the overall surface area of a particle at the microlevel. As illustrated in the figure, stabilized clay shows a considerable drop in surface area (from 45 to 22 m²/g) during the first 28 aging days, with minimal additional change seen from 28 to 60 days (from 22 to 18 m²/g). Also, a considerable reduction in surface area (from 45 to 39 m²/g) was interestingly detected after only seven aging days. The analysis of changes in the surface area suggested that the biopolymer treatment reduced the outside surface area by filling the voids in treated soil with new hydrogels (Latifi et al. 2015). As shown in the SEM micrographs, this change in a surface area correlates to the chemical or physical alteration of the natural soil into a newly cemented and engineered geomaterial with a dense-flocculated structure.

Table 3 Prediction models for percent decrease in swell-consolidation parameters

Parameter	Prediction Model	R ²	Correlation Coefficient	Significance F
Compression index, C_c	$\Delta C_c = 15.8 + 1.9 \times XG + 1.1 \times d$	0.80	0.94	1.1E-07
Rebound index, C_s	$\Delta C_s = 25.2 + 2.8 \times XG + 0.9 \times d$	0.84	0.90	9.5E-07
Swell, S_w (%)	$\Delta S_w = 16.1 + 2.8 \times XG + 1.0 \times d$	0.88	0.94	1.3E-13
Swell pressure, S_p (kPa)	$\Delta S_p = 26 + 1.9 \times XG + 1.1 \times d$	0.82	0.89	3.4E-08

XG in percentage of xanthan gum (0.5–5.0%), d = aging days (0–60 days)

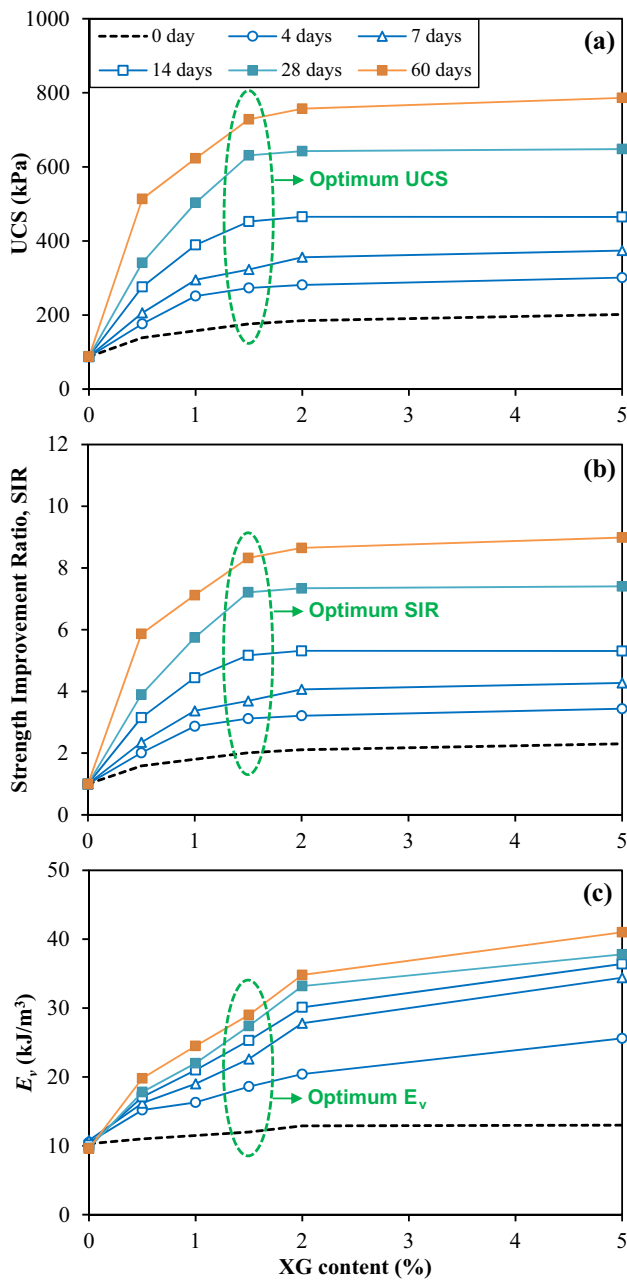


Fig. 7 a UCS, b SIR, and c E_v at different aging periods in unconfined shear tests

Soil-XG strengthening mechanism

Figure 9 shows the SEM micrographs of 28 days aged treated samples to determine the micro-mechanics of soil stabilization, with EDX analysis to determine the elemental composition of soil with varying XG contents. The micrographs reveal that the soil voids were not filled with XG-gel at 0.5 percent XG, resulting in lower strength gain values previously observed. At 1.5 percent XG and above, the biopolymer molecules were able to

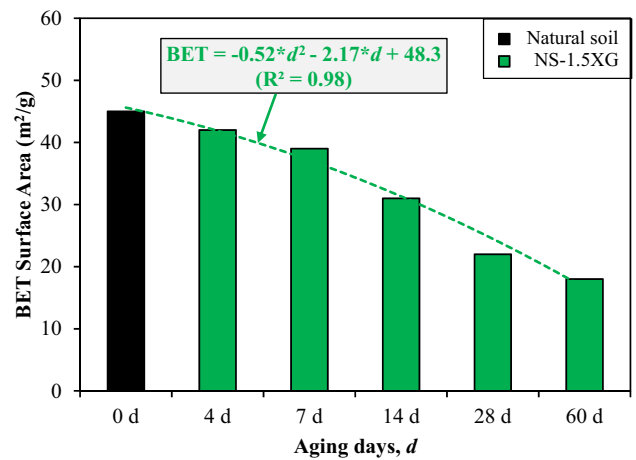
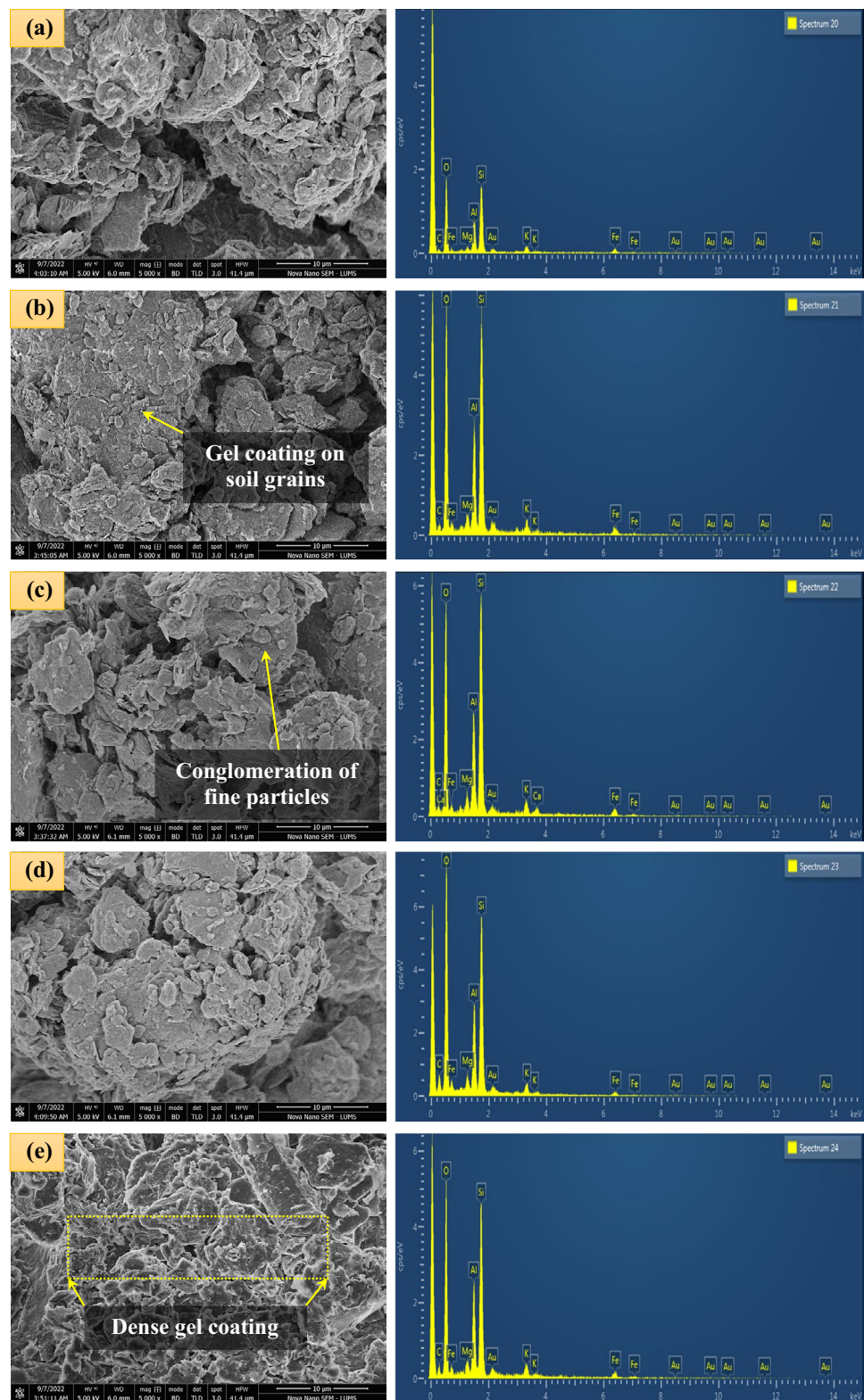


Fig. 8 BET test results for untreated and stabilized specimens

fill the voids and coat the soil grains with dense hydrogels, resulting in dense flocculation of clay particles and enhanced strength. The significant difference in soil SEM micrograph appearance is attributed to the hydrated XG gel covering. In contrast, when the biopolymer surpasses the 1.5% XG optimal level, the soil fabric shows a more conglomerated matrix with more significant inter/intra assemblage voids. EDX analysis also proved the formation of cementitious hydrogels and cross-link elements in the soil fabric. High peaks represent a greater quantity of that element present in a sample. The peak intensities of xanthan gum-clay mixtures differed from the peak intensities of natural soil and pure xanthan gum. Instead, it was stipulated that both the places and values of peaks differed from those of natural soil and pure xanthan gum (Bağrıaçık and Mahmutluoğlu 2021). This phenomenon demonstrates that when the mixing of XG and soil was completed, strength improvements occurred in the peak intensities due to a chemical reaction between soil grains and XG particles, resulting in better bonding properties of the soil-XG composite. After an aging period of 60 days, more hydrogel formation has been observed in the soil system, shown in Fig. 10. The observed micrographs offer practical reasoning for the substantial decrease in swell-consolidation properties, permeability decrement, and considerable enhancement in freeze–thaw durability. The schematic diagram between clay grains and XG biopolymer is also illustrated in Fig. 11. Direct interactions (electrostatic or hydrogen bonding) between xanthan gum monomers and clay grains occur due to electrically charged clay grains in the soil fabric (Barani and Barfar 2021). These XG monomers form inter-connected cation bridges between individual grains, cover their surfaces with a thick gel, and increase the contact area between grains.

Fig. 9 SEM and EDX graphs of XG-treated soil (**a** 0.5%, **b** 1%, **c** 1.5%, **d** 2%, and **e** 5% XG) at 28 aging days

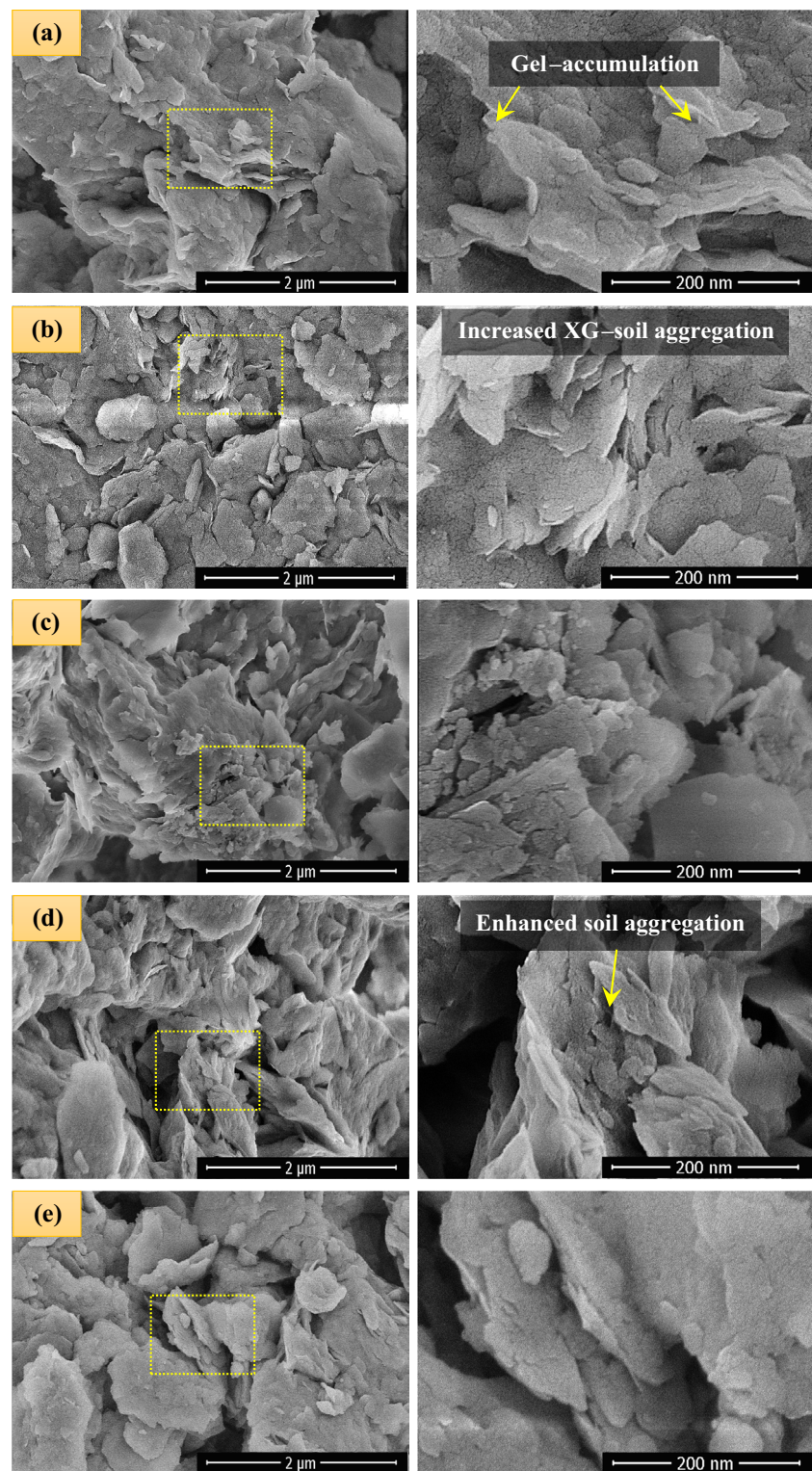


Prediction models for UCS and E_v of treated soil

Based on the shear strength test results presented in this study, regression analysis was performed to develop

prediction models for the percentage increase in UCS and E_v of treated soil shown in Fig. 12 and Table 4. The proposed prediction models fit the observed data well, with respective R^2 values of 85 and 89 percent. The significance F value for

Fig. 10 SEM images of XG-treated soil (**a** 0.5%, **b** 1%, **c** 1.5%, **d** 2%, and **e** 5% XG) at 60 aging days



this model is acceptably less than the maximum boundary limit (≤ 0.05). It has also been observed that about 96% of the data points fall within the range of 90% upper–lower prediction bands, which indicates an acceptably good prediction model.

Hydraulic conductivity of XG-strengthened soil

The ability of a geomaterial to allow water molecules to flow through it is termed hydraulic conductivity. Figure 13 summarizes the changes in stabilized soil's hydraulic

Fig. 11 Schematic diagram illustrating the interaction model between clay-XG particles

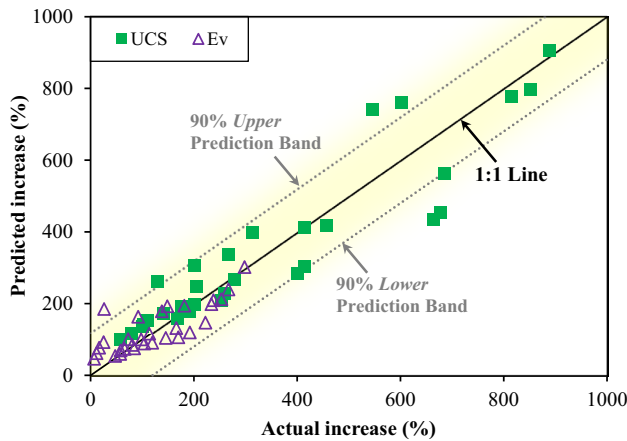
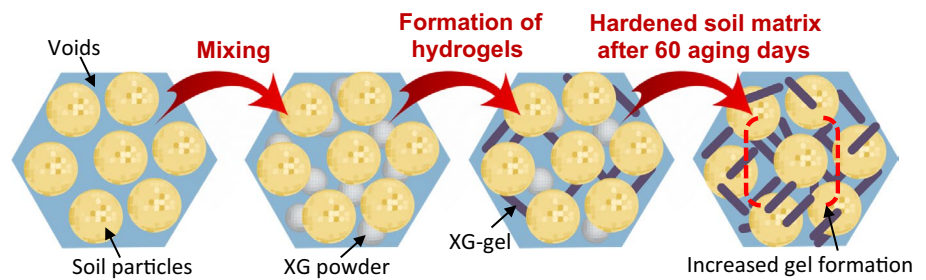


Fig. 12 Prediction models for strength parameters of treated soil

conductivity (k) during aging and indicates that the hydraulic conductivity gets significantly reduced with the increased XG concentration. At initial aging, hydraulic conductivity of natural soil was significantly reduced by 61 percent (from 230×10^{-7} to 90×10^{-7} cm/s) when stabilized with 1.5 percent XG and further reduced to 80 percent with 5 percent XG content. The production of hydrogels in the soil fabric prevents the water flow through the gaps as the biopolymer content increases (Singh and Das 2020). The reduction rate of k values becomes much more prominent with prolonged aging. The addition of 1.5 percent xanthan gum to the soil reduced the k value by 85 percent (from 230×10^{-7} to 35×10^{-7} cm/s) at four aging days and further reduced it to 90, 95, 97, and 98 percent for 7, 14, 28, and 60 days of aging, respectively. A similar trend has been observed for soil with 5 percent XG. The

k values decrease with increased XG dosage due to filling up the available voids with gum particles. Researchers (Cabalar et al. 2017; Biju and Arnepalli 2020; Sujatha et al. 2021) also report similar observations.

The decreasing trend of k with increasing aging days implies that chemical reactions like pore-clogging, crosslinking elements, and hydrogel formation persist over time. For all percentages of biopolymer examined, k decreases with increasing XG content and aging, and this also supports the concept that the biopolymer has not degraded in the soil matrix over the 60-days study period. The lower k of soil-biopolymers have potential uses in contaminant and seepage barriers, grouting material, slurry walls, landfill liners, etc.

Effect of XG on cohesion and internal friction angle of soil

The cohesion (c) and internal friction angle (ϕ) of xanthan gum-amended clay were investigated using direct shear box testing for pseudo-strain measurement. Under the same conditions, a series of interface direct shear tests were carried out and compared to the shear results of natural soil (soil-to-soil shearing). Direct shear test device Humboldt HM-5750D.3F was used to test all samples. Figure 14 demonstrates the improvement of soil's cohesion and angle of internal friction treated with different XG contents. The c values show a well-defined rise with the increase in XG content and aging periods, along with the progressive increment of ϕ values as XG content increases. There is an increasing relationship between c , ϕ , XG content, and aging time. As an example, the soil containing 5 percent XG presented a c value of 108.6 kPa and ϕ of 21° after 60 aging days, whereas

Table 4 Prediction models for percent decrease in strength parameters

Parameter	Prediction Model	R ²	Correlation Coefficient	Significance F
Unconfined compressive strength, UCS	$\Delta UCS = 80.3 + 36.4 \times XG + 10.7 \times d$	0.85	0.92	6.2E-12
Energy Absorption capacity, E_v	$\Delta E_v = 30.6 + 30.8 \times XG + 1.9 \times d$	0.89	0.94	1.3E-07

XG in percentage of xanthan gum (0.5–5.0%), d = aging days (0–60 days)

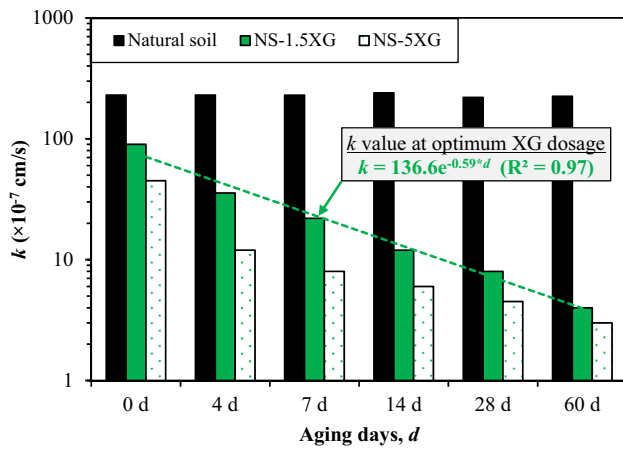


Fig. 13 Variation in hydraulic conductivity of xanthan gum-treated soil with aging

the immediately tested soil showed a c value of 67.4 kPa and ϕ of 17.4° . As a result, the respective increase in cohesion and internal friction angle values were determined to be around twofold increase.

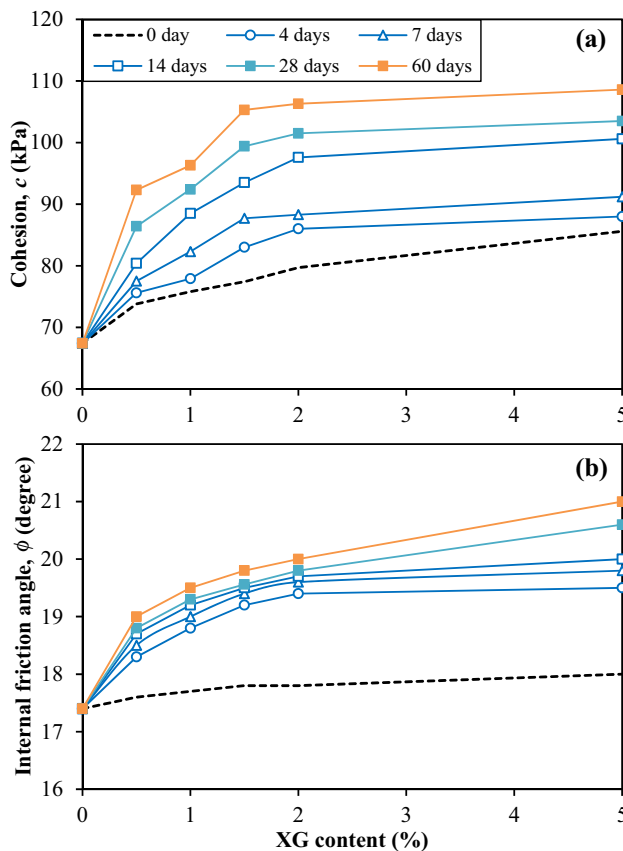


Fig. 14 **a** Cohesion, and **b** angle of internal friction of soil in direct shear tests

A strong network of hydrogen bonding might be formed between the soil particles and xanthan gum biopolymers. Lower quantities of xanthan gum inhibited contact with soil grains by filling the voids in soil fabric, resulting in a slight reduction in maximum shear strength. Higher XG contents in the mixtures can either enhance the shear strength or decrease it, depending on the amount of applied vertical force (Cabalar et al. 2018). Similar observations have been observed for direct shear results by some researchers (Cabalar et al. 2018; Latifi et al. 2017; Latifi et al. 2016a, b).

Prediction models for c and ϕ of treated soil

Based on the direct shear strength test results presented in this study, regression analysis was performed to develop prediction models for the percentage increase in cohesion and internal friction angle of treated soil as shown in Fig. 15 and Table 5. The proposed prediction models fit the observed data well, with respective R^2 values of 83 and 88 percent. The significance F value for this model is acceptably less than the maximum boundary limit (≤ 0.05). It has also been observed that about 96% of the data points fall within the range of 90% upper–lower prediction bands, which indicates an acceptably good prediction model.

Freeze–Thaw durability of XG-strengthened soil

Figure 16 shows the cumulative variation in moisture content and mass losses in soil specimens containing 0%, 0.5%, 1%, and 1.5% XG contents. Weathering and decomposition are observable phenomena in geotechnical engineering (Singh and Das 2020). XG biopolymer shows greater stability under severe conditions such as alkaline and acidic environment, thermo-decomposition below 250°C , and oxidation (Muguda et al. 2017). A freeze–thaw test was performed

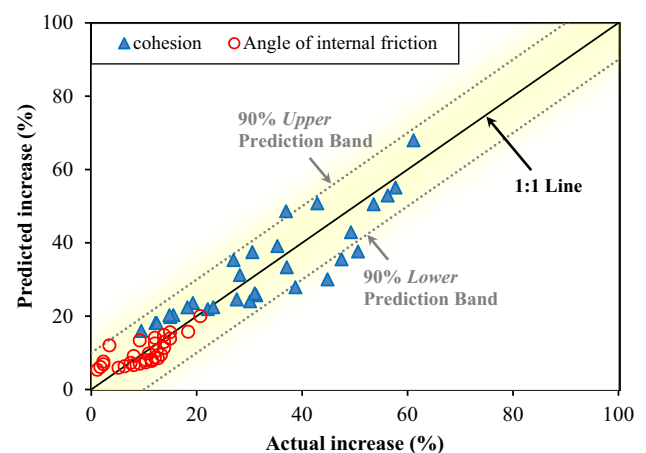


Fig. 15 Prediction models for cohesion and angle of internal friction of treated soil

Table 5 Prediction models for percent increase in DS parameters of soil

Parameter	Prediction Model	R ²	Correlation Coefficient	Significance F
Cohesion, <i>c</i>	$\Delta c = 13.8 + 4.3 \times XG + 0.5 * d$	0.83	0.91	1.0E-09
Angle of internal friction, ϕ	$\Delta \phi = 4.6 + 1.4 \times XG + 0.1 * d$	0.88	0.93	1.2E-05

XG in percentage of xanthan gum (0.5–5.0%), *d* = aging days (0–60 days)

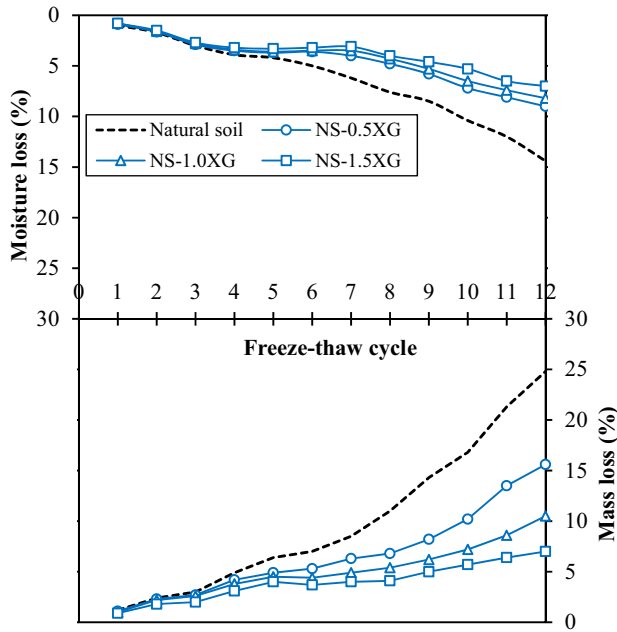


Fig. 16 Cumulative changes in moisture content and mass losses with freeze–thaw cycles

to determine the durability of the biopolymer under harsh environmental conditions. The test results indicate that the cumulative variation in moisture loss and mass loss in XG-treated specimens is substantially smaller than untreated soil. The rheology of the XG-treated soil is changed due to an increase in pore fluid viscosity, which supports the soil's ability to resist moisture loss and retain moisture. A considerable reduction in mass loss is also found in treated

samples due to the sticky interaction of XG strands with soil grains. The long-chain polymer network of biopolymer absorbs adequate water due to hydrogen bonding forming a thin coating around the soil particles improving their binding ability. Highly plastic silts treated with 1% XG showed improved moisture retention capacity with 12 freeze/thaw cycles. The ability of XG biopolymer-stabilized clays in resisting weathering action ascertains their use for erosion control applications along slopes.

Economic feasibility of XG biopolymer for soil stabilization

To prepare the way for the long-term use of XG as an expansive soil stabilizer, a brief economic and environmental feasibility comparison with a widely used conventional cement additive was made. Because of their commercial availability, biopolymers in soil stabilization might give an alternative for green and cost-effective building. According to the research, XG uses approximately 4.97 kg of CO₂ every kilograms of biopolymer (Mohanty et al. 2002). Table 6 briefly compares the treatment of one ton of problematic soil. The material prices were calculated using market rates in Punjab Province, Pakistan. The XG stabilization was shown to be superior in terms of environmental effect (i.e., CO₂ consumption) and cost when compared to cement stabilization for the treatment of one-ton soil. Overall, considering its multiple benefits over typical admixtures, XG stabilization as a green building material might provide a sustainable option.

Table 6 Economic feasibility comparison of XG stabilization with cement treatment

Soil stabilization material	Unit	Cement	Xanthan gum
The market price of material	USD/ton	450	2400
Amount required for 1-ton soil treatment	kg	80 kg (@8%/ton of soil)	15 kg (@1.5%/ton of soil)
Material price for 1-ton soil treatment	USD	36	36
CO ₂ emission per 1-kg material production	kg CO ₂	+1.24	– 4.95
CO ₂ emission related to 1-ton soil treatment	kg CO ₂	+126	– 24.76
CO ₂ emission trade related to 1-ton soil treatment ^a	USD	+2.67	– 0.57
Total cost for 1-ton soil treatment (with carbon trade exchange considerations)	USD	38.6	35.4

^aEuropean Union Emission Trading Scheme (EU–ETS) carbon emission trade (2012) [ec.europa.eu].

Applications of xanthan gum in geotechnical engineering

The previous researches have indicated that the xanthan gum can be utilized in nearly all engineering applications, including embankments, pavement construction, slope stability, retaining wall backfill, foundation soils, and swell potential mitigation. The use of XG biopolymer (non-traditional stabilizer) is one of the promising green solutions as it shows better strengthening ability for use with different soil types in geotechnical engineering practices (Lee et al. 2019). The advantages of XG-stabilized soil include ecological benefits, ease of labor, execution speed, availability, high resistance to biodegradation, and suitability to be used in all weather conditions. XG is very cost-competitive when compared to other traditional materials because, unlike different chemical stabilization procedures, the construction operation of XG-stabilized clay is unaffected by climate conditions (Li 2005). Hence, eco-friendly xanthan gum biopolymer may lead to the more prevalent usage of XG-stabilized soil and more profitable construction in the geotechnical engineering field.

Conclusions

The following conclusions have been drawn from this study:

- The max dry density of soil gets slightly reduced with biopolymeric inclusions due to its low specific gravity of 1.1, while the optimum moisture content of treated soil increased by 13 percent due to hydrophilic nature of xanthan gum biopolymer.
- The unconfined compressive strength (*UCS*), strength improvement ratio (*SIR*), and energy absorption capacity (E_v) of pure soil enhanced by 4–9 folds increase with the XG biopolymeric inclusions, although this strength increment was sustained up to 5% XG content. However, the maximum increment in shear strength parameters was recorded at 1.5% XG and aging time of 60 days. This strength enhancement could be due to the hydro-gelling effect and development of cross-linking elements in the soil matrix with prolonged aging as a result of microscopic soil-XG particles interaction. The hydraulic conductivity (*k*) and *BET* surface area were also decreased by 98 and 60 percent, respectively, due to the pore-clogging ability of XG gels in soil fabric.
- With the increase in aging time and XG content, the consolidation properties (C_c , C_s) values were found to be increased by 78 percent at 60 aging days. The swell potential parameters (S_p , S_w) were also significantly mitigated by 79 and 84 percent, respectively, with optimal

biopolymer dosage of 1.5% XG. Hence, the treated soil is shifted from high-expansivity to low-expansivity class.

- Likewise, the direct shear strength tests conducted on 1.5% XG-treated samples showed considerable increment in cohesion (*c*) by 306 percent and angle of internal friction (ϕ) by 12 percent, due to the phenomenon already explained before.
- The adhesive interaction of XG with soil grains results in a significant decrease in moisture loss by 51% and mass loss by 72% in the freeze–thaw durability test. The ability of XG-stabilized clays to resist weathering action enables their use for erosion control applications along slopes.
- Scanning electron microscopy (SEM) coupled with energy-dispersive X-ray (EDX) data corroborated the formation of hydrogels and cross-link elements inside the soil matrix. These hydrogel elements firmly weld the soil particles together, fill the pore spaces, and reduce the *BET* surface area of soil particles up to great extent.

Acknowledgements The authors gratefully acknowledge the laboratory and technical support provided by the Geotechnical Engineering Laboratory at the School of Civil Engineering, Central South University, Changsha, China, College of Civil Engineering, Tongji University, and the University of Lahore, Lahore, Pakistan.

Author contributions MH contributed to conceptualization, validation, formal analysis, investigation, writing—original draft, review, and editing. ZN performed supervision, project administration, review, and editing. Mubashir Aziz performed visualization, formal analysis, review, and editing. NI contributed to conceptualization, validation, formal analysis, investigation, writing—original draft, review, and editing. OA contributed to methodology, software, review, and editing. CF performed visualization, formal analysis, review, and editing. MUG contributed to methodology, software, validation, review, and editing. ZI contributed to conceptualization, investigation, writing—original draft, review, and editing. SN performed supervision, project administration, review, and editing. MFM contributed to methodology, software, validation, review, and editing.

Funding The authors declare that no funds, grants, or other support were received during the preparation of this manuscript.

Data availability statement Authors can confirm that all relevant data are included in the article and/or its supplementary information files.

Declarations

Conflict of interest The authors have no relevant financial or non-financial interests to disclose.

References

- ASTMD698-12 (2021) Standard test methods for laboratory compaction characteristics of soil using standard effort (12,400 ft-lbf/ft³ (600 kN-m/m³)). ASTM International, West Conshohocken







- ASTMD1557-12e1 (2012) Standard test methods for laboratory compaction characteristics of soil using modified effort (56,000 ft-lbf/ft³ (2,700 kN-m/m³)). ASTM International, West Conshohocken
- ASTM D2166M (2016M) Standard test method for unconfined compressive strength of cohesive soil. ASTM International, West Conshohocken
- ASTMD3080 (2011) Standard test method for direct shear test of soils under consolidated drained conditions. ASTM International, West Conshohocken
- ASTMD2435M-11 (2011M) Standard test methods for one-dimensional consolidation properties of soils using incremental loading. ASTM International, West Conshohocken
- ASTM D5084 (2016) Standard test methods for measurement of hydraulic conductivity of saturated porous materials using a flexible wall permeameter. ASTM International, West Conshohocken
- ASTM D560 (2012) ASTM D560–96 Standard test methods for freezing and thawing compacted soil-cement mixtures. ASTM Int, Cham, pp 1–6
- Acharya R, Pedarla A, Bheemasetti TV, Puppala AJ (2017) Assessment of guar gum biopolymer treatment toward mitigation of desiccation cracking on slopes built with expansive soils. *Transp Res Rec* 2657:78–88
- Ali M, Aziz M, Hamza M, Madni MF (2020) Engineering properties of expansive soil treated with polypropylene fibers. *Geomech Eng* 22:227–236. <https://doi.org/10.12989/gae.2020.22.3.227>
- Anandha Kumar S, Sujatha ER (2021) Assessing the potential of xanthan gum to modify in-situ soil as baseliners for landfills. *Int J Environ Sci Technol*. <https://doi.org/10.1007/s13762-021-03721-4>
- Arasan S, Bagherinia M, Akbulut RK, Zaimoglu AS (2017) Utilization of polymers to improve soft clayey soils using the deep mixing method. *J Environ Eng Geosci* 23:1–12. <https://doi.org/10.2113/gsegeosci.23.1.1>
- Ayeldeen MK, Negm AM, El Sawwaf MA (2016) Evaluating the physical characteristics of biopolymer/soil mixtures. *Arab J Geosci* 9:371. <https://doi.org/10.1007/s12517-016-2366-1>
- Ayeldeen M, Negm A, El-Sawwaf M, Kitazume M (2017) Enhancing mechanical behaviors of collapsible soil using two biopolymers. *J Rock Mech Geotech Eng* 9:329–339. <https://doi.org/10.1016/j.jrmge.2016.11.007>
- Aziz M (2020) Using grain size to predict engineering properties of natural sands in Pakistan. *Geomech Eng* 22:165–171. <https://doi.org/10.12989/gae.2020.22.2.165>
- Aziz M, Hamza M, Rasool AM, et al (2022) Use of Graphene Oxide Nanomaterial to Improve Mechanical Properties of Cement-Treated Silty Soil. *Arab J Sci Eng* 1–16. <https://doi.org/10.1007/s13369-022-07530-w>
- Aziz M, Sheikh FN, Qureshi MU et al (2021) Experimental study on endurance performance of lime and cement-treated cohesive soil. *KSCE J Civ Eng* 25:3306–3318. <https://doi.org/10.1007/s12205-021-2154-7>
- Bağrıaçık B, Mahmutluoğlu B (2021) Model experiments on coarse-grained soils treated with xanthan gum biopolymer. *Arab J Geosci*. <https://doi.org/10.1007/S12517-021-08134-8>
- Barani OR, Barfar P (2021) Effect of xanthan gum biopolymer on fracture properties of clay. *J Mater Civ Eng* 33:4020426. [https://doi.org/10.1061/\(ASCE\)MT.1943-5533.0003526](https://doi.org/10.1061/(ASCE)MT.1943-5533.0003526)
- Biju MS, Arnepalli DN (2020) Effect of biopolymers on permeability of sand-bentonite mixtures. *J Rock Mech Geotech Eng* 12:1093–1102. <https://doi.org/10.1016/j.jrmge.2020.02.004>
- Cabalar AF, Wiszniewski M, Skutnik Z (2017) Effects of xanthan gum biopolymer on the permeability, odometer, unconfined compressive and triaxial shear behavior of a sand. *Soil Mech Found Eng* 54:356–361. <https://doi.org/10.1007/S11204-017-9481-1>
- Cabalar AF, Awraheem MH, Khalaf MM (2018) Geotechnical properties of a low-plasticity clay with biopolymer. *J Mater Civil Eng* 30:4018170. [https://doi.org/10.1061/\(ASCE\)MT.1943-5533.0002380](https://doi.org/10.1061/(ASCE)MT.1943-5533.0002380)
- Chang I, Cho G-C (2019) Shear strength behavior and parameters of microbial gellan gum-treated soils: from sand to clay. *Acta Geotech* 14:361–375. <https://doi.org/10.1007/s11440-018-0641-x>
- Chang I, Im J, Prasadhi AK, Cho GC (2015) Effects of xanthan gum biopolymer on soil strengthening. *Constr Build Mater* 74:65–72. <https://doi.org/10.1016/j.conbuildmat.2014.10.026>
- Chang I, Im J, Cho GC (2016) Introduction of microbial biopolymers in soil treatment for future environmentally-friendly and sustainable geotechnical engineering. *Sustain* 8:251. <https://doi.org/10.3390/su8030251>
- Chen R, Zhang L, Budhu M (2013) Biopolymer stabilization of mine tailings. *J Geotech Geoenvironmental Eng* 139:1802–1807. [https://doi.org/10.1061/\(asce\)gt.1943-5606.0000902](https://doi.org/10.1061/(asce)gt.1943-5606.0000902)
- Chen R, Lee I, Zhang L (2015) Biopolymer stabilization of mine tailings for dust control. *J Geotech Geoenviron Eng* 141:4014100
- Chen C, Wu L, Perdjon M et al (2019) The drying effect on xanthan gum biopolymer treated sandy soil shear strength. *Constr Build Mater* 197:271–279. <https://doi.org/10.1016/j.conbuildmat.2018.11.120>
- Chenu C (1993) Clay- or sand-polysaccharide associations as models for the interface between micro-organisms and soil: water related properties and microstructure. *Geoderma* 56:143–156. [https://doi.org/10.1016/0016-7061\(93\)90106-U](https://doi.org/10.1016/0016-7061(93)90106-U)
- Comba S, Sethi R (2009) Stabilization of highly concentrated suspensions of iron nanoparticles using shear-thinning gels of xanthan gum. *Water Res* 43:3717–3726. <https://doi.org/10.1016/j.watres.2009.05.046>
- Congress IR (2015) Guidelines for the design of flexible pavements for low volume rural roads. IRC SP 72–2015
- Das BM, Sobhan K (2013) Principles of Geotechnical Engineering, 8th edn. Cengage Learning, Stamford
- Day RW (2006) Foundation engineering handbook: design and construction with the 2006 international building code. McGraw-Hill
- Dehghan H, Tabarsa A, Latifi N, Bagheri Y (2019) Use of xanthan and guar gums in soil strengthening. *Clean Technol Environ Policy* 21:155–165. <https://doi.org/10.1007/s10098-018-1625-0>
- Elkafoury A, Azzam W (2021) Utilize Xanthan gum for enhancing CBR value of used cooking oil-contaminated fine sand subgrade soil for pavement structures. *Innov Infrastruct Solut*. <https://doi.org/10.1007/s41062-020-00389-6>
- García-Ochoa F, Santos VE, Casas JA, Gómez E (2000) Xanthan gum: production, recovery, and properties. *Biotechnol Adv* 18:549–579. [https://doi.org/10.1016/S0734-9750\(00\)00050-1](https://doi.org/10.1016/S0734-9750(00)00050-1)
- Hamidi A, Hooresfand M (2013) Effect of fiber reinforcement on triaxial shear behavior of cement treated sand. *Geotext Geomembr* 36:1–9. <https://doi.org/10.1016/j.geotextmem.2012.10.005>
- Hamza M, Aziz M, Xiang W et al (2022a) Strengthening of high plastic clays by geotextile reinforcement. *Arab J Geosci* 15:805. <https://doi.org/10.1007/s12517-022-09972-w>
- Hamza M, Ijaz N, Fang C, Ijaz Z (2022b) Stabilization of Problematic Expansive Clays Using Polypropylene Fiber Reinforcement. *Jordan J Civil Eng* 16:531–539
- Hamza M, Nie Z, Aziz M et al (2022c) Geotechnical properties of problematic expansive subgrade stabilized with xanthan gum biopolymer. *Road Mater Pavement Des*. <https://doi.org/10.1080/14680629.2022.2092027>
- Hamza M, Nie Z, Aziz M et al (2022d) Strengthening potential of xanthan gum biopolymer in stabilizing weak subgrade soil. *Clean Technol Environ Policy*. <https://doi.org/10.1007/s10098-022-02347-5>
- Holtz WG, Gibbs HJ (1956) Engineering properties of expansive clays. *Trans Am Soc Civ Eng* 121:641–663. <https://doi.org/10.1061/TACEAT.0007325>

- Ijaz N, Dai F, Meng L et al (2020) Integrating lignosulphonate and hydrated lime for the amelioration of expansive soil: a sustainable waste solution. *J Clean Prod* 254:119985. <https://doi.org/10.1016/j.jclepro.2020.119985>
- Ijaz N, Rehman ur Z, Ijar Z (2022a) Recycling of paper/wood industry waste for hydromechanical stability of expansive soils: a novel approach. *J Clean Prod* 348:131345. <https://doi.org/10.1016/j.jclepro.2022.131345>
- Ijaz N, Ye W, Rehman ur Z et al (2022b) New binary paper/wood industry waste blend for solidification/stabilisation of problematic soil subgrade: macro-micro study. *Road Mater Pavement Des.* <https://doi.org/10.1080/14680629.2022.2064905>
- Ingles OG, Metcalf JB (1972) Soil stabilization: principles and practice. Soil stabilization: principles and practice. Springer, Cham, p 374
- Kumara SA, Sujatha ER (2020) Performance evaluation of β -glucan treated lean clay and efficacy of its choice as a sustainable alternative for ground improvement. *Geomech Eng* 21:413–422. <https://doi.org/10.12989/gae.2020.21.5.413>
- Kwon Y-M, Chang I, Lee M, Cho G-C (2019) Geotechnical engineering behavior of biopolymer-treated soft marine soil. *Geomech Eng* 17:453–464. <https://doi.org/10.12989/gae.2019.17.5.453>
- Latifi N, Marto A, Eisazadeh A (2015) Analysis of strength development in non-traditional liquid additive-stabilized laterite soil from macro-and micro-structural considerations. *Environ Earth Sci* 73:1133–1141. <https://doi.org/10.1007/s12665-014-3468-2>
- Latifi N, Horpibulsuk S, Meehan CL et al (2016a) Xanthan gum biopolymer: an eco-friendly additive for stabilization of tropical organic peat. *Environ Earth Sci.* <https://doi.org/10.1007/s12665-016-5643-0>
- Latifi N, Rashid ASA, Marto A, Tahir MM (2016b) Effect of magnesium chloride solution on the physico-chemical characteristics of tropical peat. *Environ Earth Sci* 75:1–9. <https://doi.org/10.1007/s12665-015-4788-6>
- Latifi N, Horpibulsuk S, Meehan CL et al (2017) Improvement of problematic soils with biopolymer—an environmentally friendly soil stabilizer. *J Mater Civ Eng* 29:04016204. [https://doi.org/10.1061/\(asce\)mt.1943-5533.0001706](https://doi.org/10.1061/(asce)mt.1943-5533.0001706)
- Lee S, Chung M, Park HM et al (2019) Xanthan gum biopolymer as soil-stabilization binder for road construction using local soil in Sri Lanka. *J Mater Civil Eng* 31:06019012. [https://doi.org/10.1061/\(ASCE\)MT.1943-5533.0002909](https://doi.org/10.1061/(ASCE)MT.1943-5533.0002909)
- Li C (2005) Mechanical response of fiber-reinforced soil. University of Texas
- McCormack DE (1976) Foundations on expansive soils. *Soil Sci Soc Am J* 40:viii–viii. <https://doi.org/10.2136/sssaj1976.0361599500400030011x>
- Moghal AAB, Vydehi KV (2021) State-of-the-art review on efficacy of xanthan gum and guar gum inclusion on the engineering behavior of soils. *Innov Infrastruct Solut* 6:1–14. <https://doi.org/10.1007/s41062-021-00462-8>
- Mohanty AK, Misra M, Drzal LT (2002) Sustainable bio-composites from renewable resources: opportunities and challenges in the green materials world. *J Polym Environ* 10:19–26. <https://doi.org/10.1023/A:1021013921916>
- Muguda S, Booth SJ, Hughes PN et al (2017) Mechanical properties of biopolymer-stabilised soil-based construction materials. *Géotechn Lett* 7:309–314. <https://doi.org/10.1680/jgele.17.00081>
- Nugent RA, Zhang G, Gambrell RP (2009) Effect of exopolymers on the liquid limit of clays and its engineering implications. *Transp Res Rec* 2101:34–43. <https://doi.org/10.3141/2101-05>
- Nugent RA, Zhang G, Gambrell RP (2011) The effect of exopolymers on the compressibility of clays. *Geo-frontiers 2011*. American Society of Civil Engineers, Reston, pp 3935–3944. [https://doi.org/10.1061/41165\(397\)402](https://doi.org/10.1061/41165(397)402)
- Petri DFS (2015) Xanthan gum: a versatile biopolymer for biomedical and technological applications. *J Appl Polym Sci.* <https://doi.org/10.1002/app.42035>
- Rosalam S, England R (2006) Review of xanthan gum production from unmodified starches by *Xanthomonas compestris* sp. *Enzyme Microb Technol* 39:197–207. <https://doi.org/10.1016/j.enzmt.2005.10.019>
- Singh SP, Das R (2020) Geo-engineering properties of expansive soil treated with xanthan gum biopolymer. *Geomech Geoengin* 15:107–122. <https://doi.org/10.1080/17486025.2019.1632495>
- Soldo A, Miletić M (2019) Study on shear strength of xanthan gum-amended soil. *Sustainability* 11:6142. <https://doi.org/10.3390/su11216142>
- Soldo A, Miletić M, Auad ML (2020) Biopolymers as a sustainable solution for the enhancement of soil mechanical properties. *Sci Rep* 10:1–13. <https://doi.org/10.1038/s41598-019-57135-x>
- Sujatha ER, Atchaya S, Sivasaran A, Keerdthe RS (2021) Enhancing the geotechnical properties of soil using xanthan gum—an eco-friendly alternative to traditional stabilizers. *Bull Eng Geol Environ* 80:1157–1167. <https://doi.org/10.1007/S10064-020-02010-7>
- Wang L, Weng Z, Liu Q et al (2021) Improving the mechanical properties of red clay using xanthan gum biopolymer. *Int J Polym Sci* 2021:1–16. <https://doi.org/10.1155/2021/1535772>
- Zamin B, Nasir H, Mehmood K et al (2021) An experimental study on the geotechnical, mineralogical, and swelling behavior of KPK expansive soils. *Adv Civ Eng* 2021:1–13. <https://doi.org/10.1155/2021/8493091>

Publisher's Note Springer Nature remains neutral with regard to jurisdictional claims in published maps and institutional affiliations.

Springer Nature or its licensor (e.g. a society or other partner) holds exclusive rights to this article under a publishing agreement with the author(s) or other rightsholder(s); author self-archiving of the accepted manuscript version of this article is solely governed by the terms of such publishing agreement and applicable law.

Authors and Affiliations

Muhammad Hamza^{1,2}  · Zhihong Nie¹  · Mubashir Aziz^{3,4}  · Nauman Ijaz⁵  · Osama Akram² · Chuanfeng Fang¹ · Muhammad Usman Ghani⁶ · Zain Ijaz⁵  · Sadaf Noshin²  · Muhammad Faizan Madni⁷

Zhihong Nie
niezhih@csu.edu.cn

Mubashir Aziz
mubashir.aziz@kfupm.edu.sa

Nauman Ijaz
nauman_ijaz99@tongji.edu.cn; nauman_ijaz99@hotmail.com

Osama Akram
osamaakram050@gmail.com

Chuanfeng Fang
194801059@csu.edu.cn

Muhammad Usman Ghani
muhammad.ghani@pwr.edu.pl

Zain Ijaz
zain@tongji.edu.cn

Sadaf Noshin
sadaf.noshin@tech.uol.edu.pk

Muhammad Faizan Madni
faizan.madni.uol@gmail.com

¹ School of Civil Engineering, Central South University, Changsha, China

² Department of Technology, University of Lahore, Lahore, Pakistan

³ Department of Civil and Environmental Engineering, King Fahd University of Petroleum and Minerals, Dhahran 31261, Saudi Arabia

⁴ Interdisciplinary Research Center for Construction and Building Materials, King Fahd University of Petroleum and Minerals, Dhahran 31261, Saudi Arabia

⁵ Key Laboratory of Geotechnical and Underground Engineering of Ministry of Education, College of Civil Engineering, Tongji University, Shanghai, China

⁶ Department of Civil and Transportation Engineering, Wroclaw University of Science and Technology, Wroclaw, Poland

⁷ Department of Civil Engineering, University of Lahore, Lahore, Pakistan